3D Nonlinear random vibrations of cable-moored offshore floating structures under wave excitations

†Kun Wang[1], Guo-Kang Er[2], Zhihui Zhu[1] and Vai Pan Iu[2]

[1]School of Civil Engineering, Central South University, Changsha, Hunan Province, China.
[2]Department of Civil and Environmental Engineering, University of Macau, Macau SAR, China.

† Presenting and corresponding author: vtkwang@csu.edu.cn

Abstract

The nonlinear random vibrations of the cable-moored floating structures under wave excitations are studied in three dimensions. One ends of four mooring cables are connected to the floating structure and the other ends are fixed to the seabed. The nonlinear equations of motions of the mooring cables are derived using the 3D cable elements which are formulated based on the extended Hamilton principle. The floating structure is simplified as a rigid body with six degrees of freedom. Then the equations of motion of the floating structure and mooring cables are formulated as a whole system through their connection conditions. In the last, the equations of motion of the whole structure under random wave excitation are analyzed numerically. The influences of different sag-to-span ratios and inclination angles of the mooring cables on the responses of the floating structure and maximum cable tensile force are studied.

Keywords: Cable-moored floating structure, random wave excitation, 3D cable elements, connection conditions.

Introduction

The cable-moored floating structures can find their applications in ocean engineering to exploit marine resources such as oil, gas and minerals. If the floating platform is subjected to horizontal excitations, the movements of floating platform can induce the geometry change of mooring cables. The geometric nonlinearity of the mooring cables plays an important role in the dynamical analysis due to their flexibility. Some researches simplified the mooring cables as linear springs [1, 2] or nonlinear springs [3, 4] to support the floating platform, which cannot reflect the real behavior and influence of the cables. A numerical approach was developed for analyzing the dynamic behavior of marine cables using lumped mass [5-8]. With this method, cables are discretized into linear segments connected by nodes and the equilibrium equations are established at each node. The mooring cables were fully modelled using the finite element method [9, 10], in which the equations of motions of the mooring cables and those of floating platform were solved separately and iteratively.

In this paper, the nonlinear random vibrations of three-dimensional floating structure and mooring system under wave excitations are studied. The nonlinear random equations of motions of the mooring cables are formulated using the 3D cable elements formulated based on the extended Hamilton principle [12]. The cable element is simplified as a flexible tension member without considering its bending and torsion stiffness because of the extremely large ratio of its length and cross-sectional dimension. The floating platform is considered as a rigid body with six degrees of freedom, i.e., three translational displacements and three rotational displacements. The equations of motions of both the floating platform and mooring system

are formulated as whole system through their connection conditions. Finally, the whole system under random wave excitation modelled using JONWSAP spectrum is solved numerically.

Problem Statement

Consider a floating structure and mooring system as shown in Figure 1. It consists of the floating platform and four catenary mooring lines C_1, C_2, C_3 and C_4. The floating platform and mooring cables are connected through four nodes *A*, *B*, *C* and *D*. *O* is the mass center of the floating platform. The other ends of the mooring cables are fixed on the seabed. w_a, w_b and w_c are the length, height and width of the floating platform, respectively. The top view and side view of the three-dimensional floating system are shown in Figure 2. The mooring cables C_1, C_2 and C_3, C_4 are symmetric about the *y*-axis in the plane x_1Oy and x_2Oy, respectively. θ, l and d are the inclination angle, inclined length and sag of the mooring cable, respectively. w_l is the length between the nodes *A* and *B*.

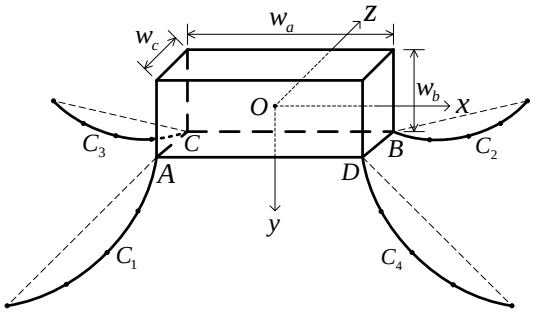

Figure 1. Configuration of the three-dimensional floating system

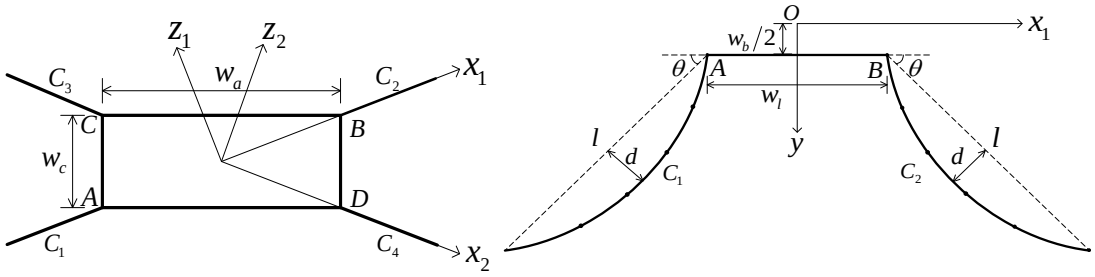

(a) (b)

Figure 2. (a) Top view (b) Side view of the three-dimensional floating system

Nonlinear Random Vibrations of the Moored Floating System

Finite Element Formulation for the Dynamics of Cable

The equations of motion for the element *e* in the local coordinate systems O-x_1yz_1 and O-x_2yz_2 are derived based on the extended Hamilton principle and they are given as follows.

$$\left(\mathbf{M}_l^e + \mathbf{M}_a^e\right)\ddot{\mathbf{d}}_l^e + \mathbf{C}_l^e\dot{\mathbf{d}}_l^e + \mathbf{K}_l^e(\mathbf{d}_l^e)\mathbf{d}_l^e = \mathbf{f}_d^e \tag{1}$$

where $\mathbf{d}_l^e$ is the displacement vector of element *e* in the local coordinate systems O-x_1yz_1 and O-x_2yz_2; $\mathbf{f}_d^e$ is drag force vector of element *e*; $\mathbf{M}_a^e$ is the added mass matrix of element *e* which is expressed as

$$\mathbf{M}_a^e = \frac{\rho_s A l^e}{2} \mathbf{T}_1^T \begin{bmatrix} 0 & 0 & 0 & 0 & 0 & 0 \\ 0 & C_c & 0 & 0 & 0 & 0 \\ 0 & 0 & C_c & 0 & 0 & 0 \\ 0 & 0 & 0 & 0 & 0 & 0 \\ 0 & 0 & 0 & 0 & C_c & 0 \\ 0 & 0 & 0 & 0 & 0 & C_c \end{bmatrix} \mathbf{T}_1 \tag{2}$$

where $\mathbf{T}_1$ is the transformation matrix between the coordinate system x_1yz_1 $\left(x_2yz_2\right)$ and the coordinate system $x_3y_3z_3$, as shown in Figure 3; C_c is the added-mass coefficient of the cable in the transverse direction.

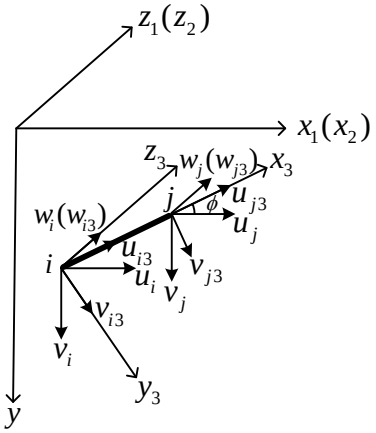

Figure 3. Differential element e in the coordinate system $x_3y_3z_3$ of the cable element and the coordinate system x_1yz_1 $\left(x_2yz_2\right)$ of the cable

With Morison's equation, the drag forces that act along the x_3, y_3, z_3 directions of element e are given as follows, respectively

$$\begin{aligned} F_{u3}^e &= -\frac{\pi}{2} \rho_s C_{dl} D_1 l^e \left(\bar{u}_3^e - V_{u3}\right)^2 \operatorname{sgn}\left(\bar{u}_3^e - V_{u3}\right) \\ F_{v3}^e &= -\frac{1}{2} \rho_s C_{dt} D_1 l^e \left(\bar{v}_3^e - V_{v3}\right)^2 \operatorname{sgn}\left(\bar{v}_3^e - V_{v3}\right) \\ F_{w3}^e &= -\frac{1}{2} \rho_s C_{dt} D_1 l^e \left(\bar{w}_3^e - V_{w3}\right)^2 \operatorname{sgn}\left(\bar{w}_3^e - V_{w3}\right) \end{aligned} \tag{3}$$

where D_1 is the diameter of the cable cross section; C_{dl} and C_{dt} are the drag coefficients in the longitudinal and transverse directions of the element e, respectively; V_{u3}, V_{v3}, V_{w3} are the fluid velocities in the x_3, y_3, z_3 directions of element e, respectively; $\bar{u}_3^e$, $\bar{v}_3^e$, $\bar{w}_3^e$ are the average velocities of element e in the x_3, y_3, z_3 directions of element e, respectively, which are expressed as

$$\bar{u}_3^e = \frac{\dot{u}_{i3} + \dot{u}_{j3}}{2}, \quad \bar{v}_3^e = \frac{\dot{v}_{i3} + \dot{v}_{j3}}{2}, \quad \bar{w}_3^e = \frac{\dot{w}_{i3} + \dot{w}_{j3}}{2} \tag{4}$$

and $\operatorname{sgn}(\bullet)$ denotes the sign function given by

$$\operatorname{sgn}(z) = \begin{cases} 1, & z > 0 \\ 0, & z = 0 \\ -1, & z < 0 \end{cases} \tag{5}$$

Therefore, the drag force vector $\mathbf{f}_d^e$ of element *e* in the coordinate system x_1yz_1 $\left(x_2yz_2\right)$ is expressed as

$$\mathbf{f}_d^e = \mathbf{T}_1^T \frac{1}{2}\left\{F_{u3}^e, F_{v3}^e, F_{w3}^e, F_{u3}^e, F_{v3}^e, F_{w3}^e\right\}^T \tag{6}$$

Using the transformation matrix $\mathbf{T}$ and the relationship $\mathbf{d}_l^e = \mathbf{T}\mathbf{d}_g^e$ in which $\mathbf{d}_g^e$ is the displacement vector of element e in the global coordinate system *O-xyz*, Eq. (1) becomes

$$\mathbf{M}_g^e\ddot{\mathbf{d}}_g^e + \mathbf{C}_g^e\dot{\mathbf{d}}_g^e + \mathbf{K}_g^e(\mathbf{d}_g^e)\mathbf{d}_g^e = \mathbf{F}_g^e \tag{7}$$

where $\mathbf{M}_g^e = \mathbf{T}^T\left(\mathbf{M}_l^e + \mathbf{M}_a^e\right)\mathbf{T}$, $\mathbf{C}_g^e = \mathbf{T}^T\mathbf{C}_l^e\mathbf{T}$, $\mathbf{K}_g^e = \mathbf{T}^T\mathbf{K}_l^e\mathbf{T}$, and $\mathbf{F}_g^e = \mathbf{T}^T\mathbf{F}_d^e$. The equations of motion of the mooring cables are

$$\mathbf{M}_m\ddot{\mathbf{U}}_m + \mathbf{C}_m\dot{\mathbf{U}}_m + \mathbf{K}_m(\mathbf{U}_m)\mathbf{U}_m = \mathbf{F}_m \tag{8}$$

where the subscript *m* denotes the number of mooring cables.

Dynamics of the Floating Platform

The floating platform has six degrees of freedom, which are displacements *u*, *v*, *w* along *x*, *y*, *z* axes and rotations *α*, *β*, *γ* in *xOy*, *xOz*, *yOz* plane, respectively. The equations of motion of the floating platform are given as follows based on Figure 4.

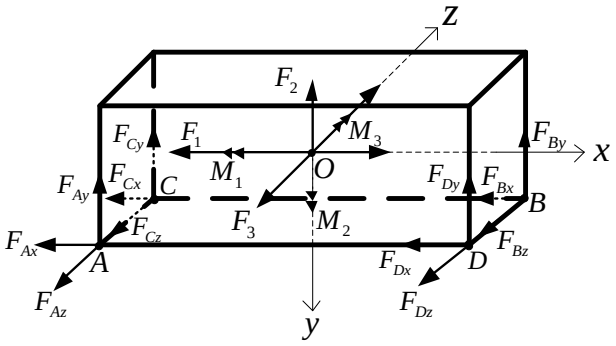

Figure 4. Forces applied on the floating platform ($F_1 = M\ddot{u} + c_4\dot{u} - F_{dx}$,
$F_2 = M\ddot{v} + c_5\dot{v} - F_{dy} + F_b$, $F_3 = M\ddot{w} + c_6\dot{w} - F_{dz}$, $M_1 = J_x\ddot{\gamma} + c_9\dot{\gamma} - M_{dx} + F_{b2}\cdot 2w_c/3$,
$M_2 = J_y\ddot{\beta} + c_8\dot{\beta} - M_{dy}$, $M_1 = J_z\ddot{\alpha} + c_7\alpha - M_{dz} + F_{b1}\cdot 2w_a/3$)

$$\sum F_x = 0: \ \left(M + M_{ax}\right)\ddot{u} + c_4\dot{u} + F_{Ax} + F_{Bx} + F_{Cx} + F_{Dx} = F_{dx} \tag{9}$$

$$\sum F_y = 0: \ \left(M + M_{ay}\right)\ddot{v} + c_5\dot{v} + F_{Ay} + F_{By} + F_{Cy} + F_{Dy} + F_b = F_{dy} \tag{10}$$

$$\sum F_z = 0: \ \left(M + M_{az}\right)\ddot{w} + c_6\dot{w} + F_{Az} + F_{Bz} + F_{Cz} + F_{Dz} = F_{dz} \tag{11}$$

$$\begin{aligned}\sum M_z = 0: J_z\ddot{\alpha} + c_7\dot{\alpha} + F_{Ax}\frac{w_b}{2} + F_{Bx}\frac{w_b}{2} + F_{Ay}\frac{w_a}{2} - F_{By}\frac{w_a}{2} + F_{Cx}\frac{w_b}{2} \\ + F_{Dx}\frac{w_b}{2} + F_{Cy}\frac{w_a}{2} - F_{Dy}\frac{w_a}{2} + F_{b1}\frac{2w_a}{3} = M_{dz}\end{aligned} \tag{12}$$

$$\begin{aligned}\sum M_y = 0: J_y\ddot{\beta} + c_8\dot{\beta} + F_{Ax}\frac{w_c}{2} - F_{Bx}\frac{w_c}{2} - F_{Az}\frac{w_a}{2} + F_{By}\frac{w_a}{2} - F_{Cx}\frac{w_c}{2} \\ + F_{Dx}\frac{w_c}{2} - F_{Cz}\frac{w_a}{2} + F_{Dz}\frac{w_a}{2} = M_{dy}\end{aligned} \tag{13}$$

$$\sum M_x = 0 : J_x\ddot{\gamma} + c_g\dot{\gamma} + F_{Ay}\frac{w_c}{2} - F_{By}\frac{w_c}{2} + F_{Az}\frac{w_b}{2} + F_{Bz}\frac{w_b}{2} - F_{Cy}\frac{w_c}{2} + F_{Dy}\frac{w_c}{2} + F_{Cz}\frac{w_b}{2} + F_{Dz}\frac{w_b}{2} + F_{b2}\frac{2w_c}{3} = M_{dx} \tag{14}$$

where M is the mass of the floating platform, M_{ax}, M_{ay}, M_{az} are the added mass of the floating platform along the x, y and z axes, respectively, which are assumed as constant because the vertical displacement is small [12]. J_z, J_y and J_x are the moment of inertia of the floating platform in the xOy, xOz and yOz planes, respectively; F_b, F_{b1} and F_{b2} are the dynamical buoyancy of the floating body; F_{Ax}, F_{Ay}, F_{Az}, F_{Bx}, F_{By}, F_{Bz}, F_{Cx}, F_{Cy}, F_{Cz}, F_{Dx}, F_{Dy}, F_{Dz} are the dynamical tensions from the cable at nodes A, B, C, and D in the x, y, z axes, respectively. F_{dx}, F_{dy}, F_{dz}, M_{dz}, M_{dy}, M_{dx} are the hydrodynamic drag forces in the x, y, z axes and xOy, xOz, yOz planes, respectively. F_b, F_{b1} and F_{b2} are the dynamical buoyancy of the floating body due to the change of submerged volume of the floating body, which are expressed as

$$\begin{aligned} F_b &= \rho_s g w_a w_c v_f \\ F_{b1} &= \frac{1}{8}\rho_s g w_a^2 w_c \alpha \\ F_{b2} &= \frac{1}{8}\rho_s g w_a w_c^2 \gamma \end{aligned} \tag{15}$$

Referring to Figure 5 with $P_1(-w_a/2, y, z)$, $P_2(w_a/2, y, z)$, $P_3(x, w_b/2, z)$, $P_4(x, y, -w_c/2)$ and $P_5(x, y, w_c/2)$, the hydrodynamic drag forces or moments that act on the floating platform are given as follows.

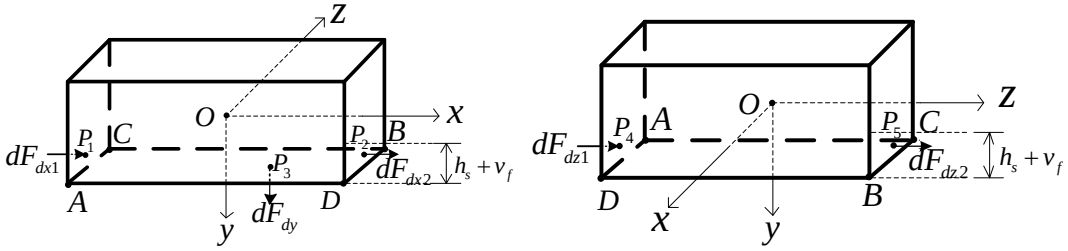

Figure 5. Drag forces act on the floating platform

$$\begin{aligned}
F_{dx} &= \int_{-w_c/2}^{w_c/2}\int_{w_b/2-h_s-v_f}^{w_b/2} dF_{x1} + \int_{-w_c/2}^{w_c/2}\int_{w_b/2-h_s-v_f}^{w_b/2} dF_{x2} \\
F_{dy} &= \int_{-w_c/2}^{w_c/2}\int_{-w_a/2}^{w_a/2} dF_y \\
F_{dz} &= \int_{-w_a/2}^{w_a/2}\int_{w_b/2-h_s-v_f}^{w_b/2} dF_{z1} + \int_{-w_a/2}^{w_a/2}\int_{w_b/2-h_s-v_f}^{w_b/2} dF_{z2} \\
M_{dz} &= \int_{-w_c/2}^{w_c/2}\int_{w_b/2-h_s-v_f}^{w_b/2} y dF_{x1} + \int_{-w_c/2}^{w_c/2}\int_{w_b/2-h_s-v_f}^{w_b/2} y dF_{x2} + \int_{-w_c/2}^{w_c/2}\int_{-w_a/2}^{w_a/2}(-x) dF_y \\
M_{dy} &= \int_{-w_c/2}^{w_c/2}\int_{w_b/2-h_s-v_f}^{w_b/2}(-z) dF_{x1} + \int_{-w_c/2}^{w_c/2}\int_{w_b/2-h_s-v_f}^{w_b/2}(-z) dF_{x2} \\
&\quad + \int_{-w_a/2}^{w_a/2}\int_{w_b/2-h_s-v_f}^{w_b/2} x dF_{z1} + \int_{-w_a/2}^{w_a/2}\int_{w_b/2-h_s-v_f}^{w_b/2} x dF_{z2} \\
M_{dx} &= \int_{-w_a/2}^{w_a/2}\int_{w_b/2-h_s-v_f}^{w_b/2} y dF_{z1} + \int_{-w_a/2}^{w_a/2}\int_{w_b/2-h_s-v_f}^{w_b/2} y dF_{z2} + \int_{-w_c/2}^{w_c/2}\int_{-w_a/2}^{w_a/2}(-z) dF_y
\end{aligned} \tag{16}$$

where dF_{dx1}, dF_{dx2}, dF_{dy}, dF_{dz1} and dF_{dz2} are expressed by

$$
\begin{aligned}
dF_{dx1} &= -\frac{1}{2}\rho_s C_{dx} dydz\left(\dot{u}_f + y\dot{\alpha} + z\dot{\beta} - V_{fx1}\right)^2 \operatorname{sgn}\left(\dot{u}_f + y\dot{\alpha} + z\dot{\beta} - V_{fx1}\right) \\
dF_{dx2} &= -\frac{1}{2}\rho_s C_{dx} dydz\left(\dot{u}_f + y\dot{\alpha} + z\dot{\beta} - V_{fx2}\right)^2 \operatorname{sgn}\left(\dot{u}_f + y\dot{\alpha} + z\dot{\beta} - V_{fx2}\right) \\
dF_{dy} &= -\frac{1}{2}\rho_s C_{dy} dxdz\left(\dot{v}_f + x\dot{\alpha} + z\dot{\gamma} - V_{fy}\right)^2 \operatorname{sgn}\left(\dot{v}_f + x\dot{\alpha} + z\dot{\gamma} - V_{fy}\right) \\
dF_{dz1} &= -\frac{1}{2}\rho_s C_{dz} dydx\left(\dot{w}_f + y\dot{\gamma} + x\dot{\beta} - V_{fz1}\right)^2 \operatorname{sgn}\left(\dot{w}_f + y\dot{\gamma} + x\dot{\beta} - V_{fz1}\right) \\
dF_{dz2} &= -\frac{1}{2}\rho_s C_{dz} dydx\left(\dot{w}_f + y\dot{\gamma} + x\dot{\beta} - V_{fz2}\right)^2 \operatorname{sgn}\left(\dot{w}_f + y\dot{\gamma} + x\dot{\beta} - V_{fz2}\right)
\end{aligned}
\tag{17}
$$

where C_{dx}, C_{dy} and C_{dz} are the drag coefficients along the x, y, and z directions, respectively; V_{fx1}, V_{fx2}, V_{fy}, V_{fz1} and V_{fz2} are the fluid velocities at specific locations along the x, y and z directions, respectively.

Formulation of the Whole System

In order to formulate the equations of motion of the mooring cables and the floating platform as a whole system, the connection conditions between the mooring lines and floating platform are required. Their relationships are

$$
\begin{aligned}
u_A &= u + \frac{w_b}{2}\alpha + \frac{w_c}{2}\beta,\ v_A = v + \frac{w_a}{2}\alpha + \frac{w_c}{2}\gamma,\ w_A = w - \frac{w_a}{2}\beta + \frac{w_b}{2}\gamma \\
u_B &= u + \frac{w_b}{2}\alpha - \frac{w_c}{2}\beta,\ v_B = v - \frac{w_a}{2}\alpha - \frac{w_c}{2}\gamma,\ w_B = w + \frac{w_a}{2}\beta + \frac{w_b}{2}\gamma \\
u_C &= u + \frac{w_b}{2}\alpha - \frac{w_c}{2}\beta,\ v_C = v + \frac{w_a}{2}\alpha - \frac{w_c}{2}\gamma,\ w_C = w - \frac{w_a}{2}\beta + \frac{w_b}{2}\gamma \\
u_D &= u + \frac{w_b}{2}\alpha + \frac{w_c}{2}\beta,\ v_D = v - \frac{w_a}{2}\alpha + \frac{w_c}{2}\gamma,\ w_D = w + \frac{w_a}{2}\beta + \frac{w_b}{2}\gamma
\end{aligned}
\tag{18}
$$

where u_A, v_A, w_A, u_B, v_B, w_B, u_C, v_C, w_C, u_D, v_D, w_D are the displacements of the nodes *A*, *B*, *C*, and *D* in the *x*, *y*, *z* axes, respectively. Then the equations of motion about the nodes *A*, *B*, *C* and *D* in Eq. (8) are removed and replaced by Eqs. (9)-(14) using the connections conditions given by Eq. (18). The variables of displacements related to nodes *A*, *B*, *C* and *D* in other equations of motion in Eq. (8) are also expressed by Eq. (18). The final equations of motion of the whole system are obtained as

$$
\mathbf{M}\ddot{\mathbf{U}} + \mathbf{C}\dot{\mathbf{U}} + \mathbf{K}(\mathbf{U})\mathbf{U} = \mathbf{F}(t) \tag{19}
$$

where $\mathbf{U}$ is the global displacement vector; $\mathbf{K}(\mathbf{U})$ is the global stiffness matrix; $\mathbf{F}(t)$ is the wave force vector.

Modeling of sea wave excitation

The sea wave is assumed to propagate in the horizontal direction in the plane *yOz*. The kinematics of the water particles under wave excitation can be calculated based on the linear Airy wave theory [13]. The free surface elevation η of the wave is introduced with a wave

spectrum $S_{\eta\eta}$. Then the surface elevation at location *z* and time *t* is expressed by using wave superposition as

$$\eta(z,t)=\sum_{i=1}^{N}\sqrt{2S_{\eta}(\omega_i)\Delta\omega}\cos(k_i z-\omega_i t+\theta_i) \tag{20}$$

where $\Delta\omega$ is the frequency interval; ω_i is the angular frequency of the *i*th wave component which equals $gk_i\tanh(k_i d)$ and *g* is the acceleration due to gravity; k_i is the *i*th wave number which equals $2\pi/\lambda_i$ and λ_i is the *i*th wavelength; *N* is the number of frequencies; θ_i is the statistically independent random phase angle which is uniformly distributed between 0 and 2π.

The condition of deep water depth is considered in this paper because $h>\lambda/2$. Therefore, the fluid velocities V_z and V_y along the *z* and *y* directions at any point *P*(*x*,*y*,*z*) and time *t* are expressed as

$$\begin{aligned}V_z&=\sum_{i=1}^{N}\sqrt{2S_{\eta\eta}(\omega_i)\Delta\omega}\omega_i e^{k_i(y+h_s-w_b/2)}\cos(k_i z-\omega_i t+\theta_i)\\ V_y&=\sum_{i=1}^{N}\sqrt{2S_{\eta\eta}(\omega_i)\Delta\omega}\omega_i e^{k_i(y+h_s-w_b/2)}\sin(k_i z-\omega_i t+\theta_i)\end{aligned} \tag{21}$$

During structural design, the significant height and average period of a random wave are specified. Therefore, the following approximate expression for the JONSWAP spectrum given by Goda [14] is adopted.

$$S_{\eta\eta}(\omega)=\alpha_1 H_s^2\frac{\omega^{-5}}{\omega_0^4}\exp\left[-1.25(\omega/\omega_0)^{-4}\right]\gamma^{\exp\left[-(\omega-\omega_0)^2/2\tau^2\omega_0^2\right]} \tag{22}$$

where

$$\alpha_1=\frac{0.0624}{0.23+0.0336\gamma-0.185(1.9+\gamma)^{-1}} \tag{23}$$

and H_s is the significant height of the wave; $\omega_0=2\pi/T_0$ is the peak angular frequency of the wave and T_0 is the average period of the wave; γ_1 is the peakedness parameter which varies from 1 to 7; and τ is a shape parameter which is expressed as

$$\tau=\begin{cases}0.07, & \omega\le\omega_0\\ 0.09, & \omega>\omega_0\end{cases} \tag{24}$$

Numerical Example

Consider a 3D cable-moored floating platform with the parameters listed in Tables 1 and 2. The density of seawater is $\rho_s=1.025\times10^3$ kg/m^3. The power spectral density $S_{\eta\eta}$ is plotted in Figure 6 with $\gamma_1=3$, $H_s=0.8$ m and $T_0=8$ s. Each cable is discretized with 11 elements because further increasing the element number cannot make the precision of the results further increased obviously. The time step is 0.0008 s and the sample size used in Monte Carlo simulation (MCS) is 10^8.

Table 1. Properties of mooring cables

Parameter	Value
Young's modulus E (N/m^2)	1.9×10^{11}
Diameter D_1 (m)	0.1
Mass density ρ (kg/m^3)	8.2×10^{3}
Damping ratio ξ	0.03
Sea depth h (m)	120
Inclination angle θ (degree)	45
Sag-to-span ratio d/l	1/90
Longitudinal drag coefficient C_{dl}	0.01
Transverse drag coefficient C_{dt}	1
Transverse added-mass coefficient C_c	1

Table 2. Properties of mooring cables

Parameter	Value
Length w_a (m)	26
Height w_b (m)	5
Width w_c (m)	10
Mass M (kg)	1.2×10^{5}
Drag coefficient C_{dx} along x axis	1
Drag coefficient C_{dy} along y axis	1
Drag coefficient C_{dz} along z axis	1

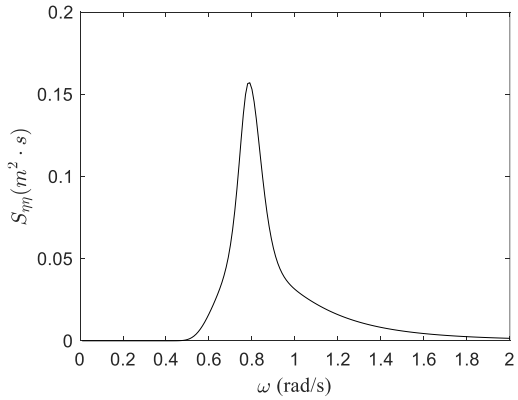

Figure 6. Power spectral density of wave surface with $\gamma_1 = 3$, $H_s = 0.8$ m and $T_0 = 8$ s

The PDFs of the responses of the floating platform and maximum cable tensile force at steady state are shown in Figure 7. The mean values of v_f, w_f, γ and T_c at steady state are 0.0059 m, 0 m, 0^o and 7.845×10^5 N, respectively and the corresponding standard deviations are 0.0112 m, 0.445 m, 1.95^o and 1.258×10^5 N.

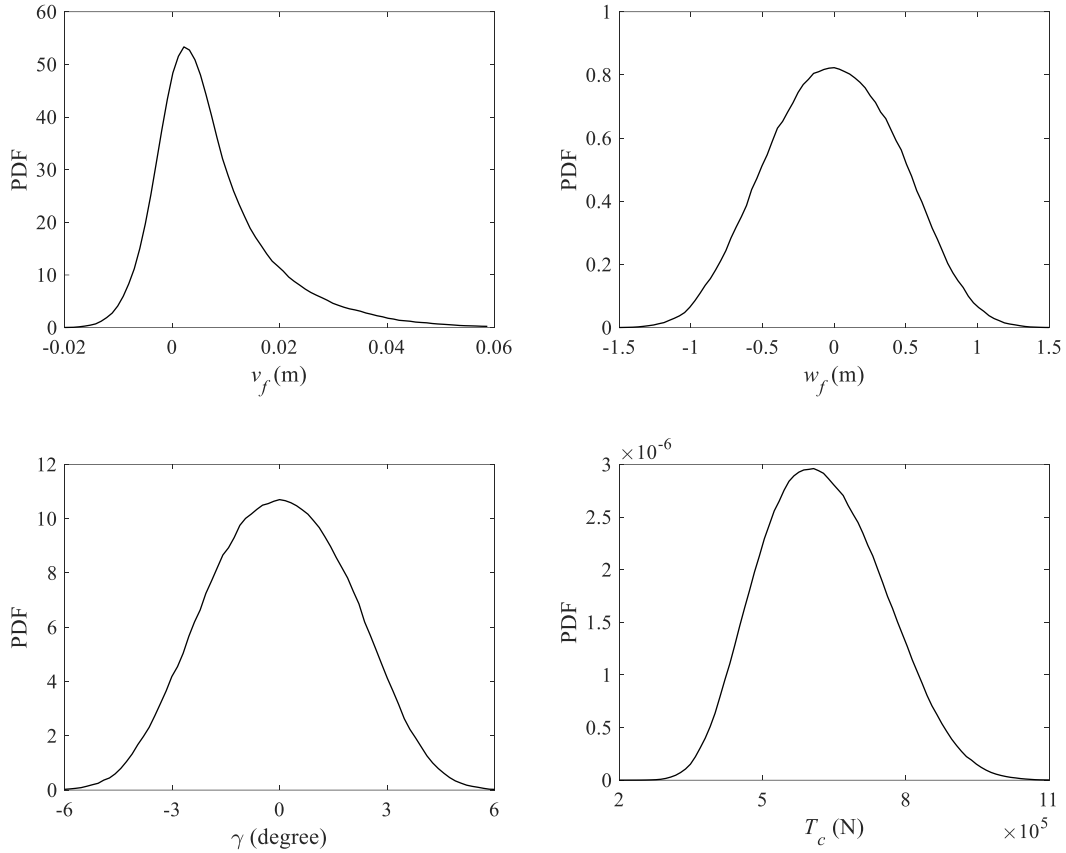

Figure 7. The PDFs of v_f, w_f, γ and T_c at steady state with $d/l = 1/90$, $\theta = 45°$

If the inclination angle of the cables keeps as 45^o, the standard deviations of the responses of the floating platform and maximum cable tensile force at steady state are shown in Figure 8. It is observed from Figure 8 that the standard deviation of w_f decreases as d/l decreases from 1/45 to 1/75. Then it increases as d/l further decreases from 1/75 to 1/150. This is due to the fact that as d/l decreases from 1/45 to 1/75, the second natural frequency of the linear system increases from 0.94 to 1.103 rad/s, which is farther away from the dominant frequency 0.79 rad/s of $S_{\eta\eta}$. As d/l decreases from 1/75 to 1/150, the fundamental natural frequency of the linear system increases from 0.586 to 0.83, which is closer to the dominant frequency of $S_{\eta\eta}$. It is also observed from that the standard deviation of v_f always decreases and the standard deviations of γ and T_c always increase as d/l decreases.

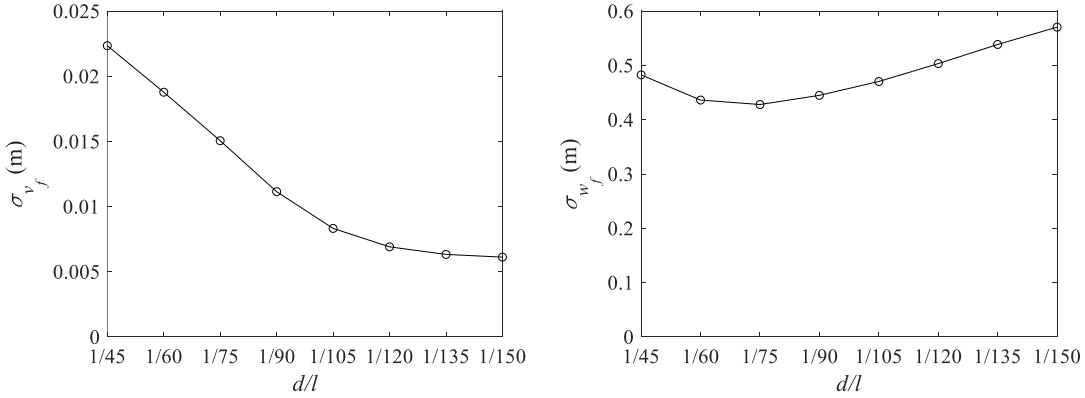

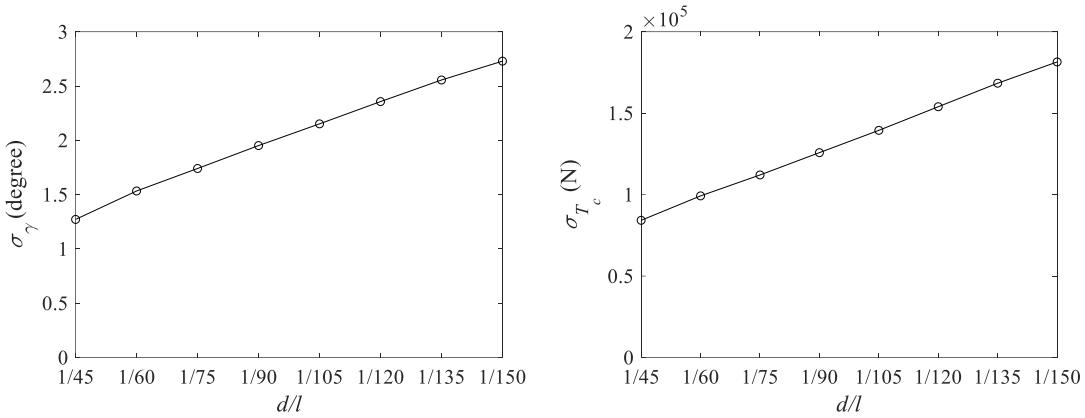

Figure 8. The standard deviations of v_f, w_f, γ and T_c at steady state for different d/l with $\theta = 45°$

If the sag-to-span ratio of the cables keeps as 1/90, the standard deviations of the responses of the floating platform and maximum cable tensile force at steady state are shown in Figure 9 for different inclination angles of the cables. It is observed from Figure 9 that the standard deviations of v_f, w_f, γ, T_c always increases as θ increases from 33^o to 54^o and they are much influenced by the inclination angles of the cables. This is due to the fact that as θ increases from 33^o to 54^o, the fundamental natural frequency of the linear system decreases from 0.679 to 0.593 rad/s and changes within a small interval, which is farther away from the dominant frequency of $S_{\eta\eta}$, but the second natural frequency of the linear system decreases from 1.576 to 0.832 rad/s, which is closer to the dominant frequency of $S_{\eta\eta}$.

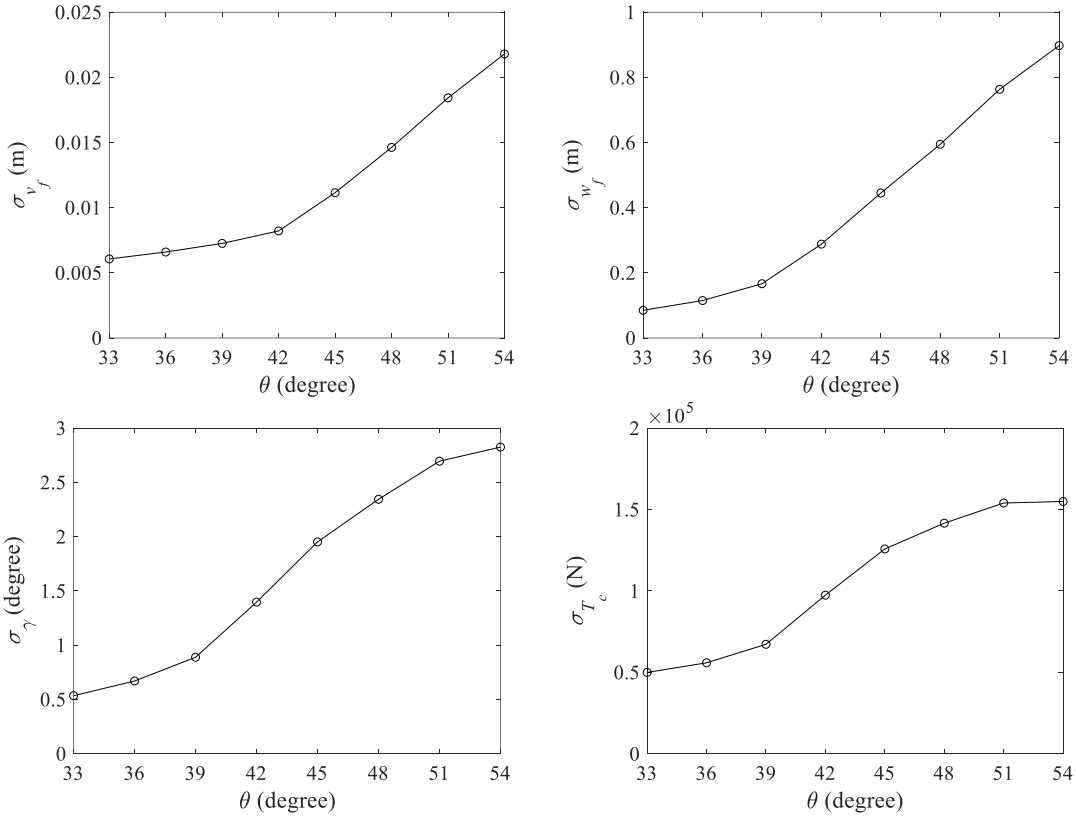

Figure 9. The standard deviations of v_f, w_f, γ and T_c at steady state for different θ with $d/l = 1/90$

Conclusions

The nonlinear random vibrations of the cable-moored offshore floating structure are analyzed under wave excitation. The floating platform is modeled as a rigid body with six degrees of freedom. The mooring cables are modeled by using the nonlinear 3D cable elements which are formulated based on the extended Hamilton principle. The effects of added-mass and nonlinear hydrodynamic drag forces on both the floating platform and mooring cables are taken into consideration. Firstly, the equations of motion of the mooring cables and floating platform are formulated separately. After that, the connection conditions between the mooring cables and floating platform are introduced to make the nonlinear equations of motions of both the mooring cables and floating platform formulated as a whole system. The equations of motion of the whole system are solved numerically using MCS. The influences of the sag-to-span ratio and inclination angle of the mooring cables on the statistical properties of the moored floating structure and the maximum cable tensile force are studied. It is found from numerical results that the responses of the floating platform and the maximum cable tensile force are much influenced by both the initial sag-to-span ratio and inclination angle of the cables.

Acknowledgement

The research work presented in this paper were obtained under the supports of the National Natural Science Foundation of China (China, Grant No. 51678576), the Research Committee of University of Macau (Grant No. MYRG2018-00116-FST) and the Science and Technology Development Fund of Macau (Grant No. 042/2017/A1).

References

[1] Yamamoto, T., Yoshida, A. and Ijima, T. (1980) Dynamics of elastically moored floating objects, *Applied Ocean Research* **2**, 85–92.

[2] Tang, H. J., Chen, C. C. and Chen, W. M. (2011) Dynamics of dual pontoon floating structure for cage aquaculture in a two-dimensional numerical wave tank, *Journal of Fluids and Structures*, 27, 918-936.

[3] Esmailzadeh, E. and Goodarzi, A. (2001) Stability ananlysis of a CALM floating offshore structure, *International Journal of Non-Linear Mechanics* **36**, 917–926.

[4] Umar, A and Datta, T. K. (2003) Nonlinear response of a moored buoy, *Ocean Engineering* **30**, 1625-1646.

[5] Huang, S. (1994). Dynamic analysis of three-dimensional marine cables. *Ocean Engineering*, **21**, 587-605.

[6] Driscoll, F. R., Lueck, R. G. and Nahon, M. (2000). Development and validation of a lumped-mass dynamics model of a deep-sea rov system. *Applied Ocean Research*, **22**, 169-182.

[7] Buckham, B., Nahon, M., Seto, M., Zhao, X. and Lambert, C. (2003) Dynamics and control of a towed underwater vehicle system, part I: model development, *Ocean Engineering* **30**, 453-470.

[8] Zhu, X. Q. and Yoo, W. S. (2016) Dynamic analysis of a floating spherical buoy fastened by mooring cables, *Ocean Engineering* 121, 462–471.

[9] Garrett, D. L. (2005) Coupled analysis of floating production system, *Ocean Engineering* **32**, 802–816.

[10] Kim, B. W., Sung, H. G., Kim, J. H. and Hong, S. Y. (2013) Comparision of linear spring and nonlinear FEM methods in dynamic coupled analysis of floating structure and mooring system, *Journal of Fluid and Structures* **42**, 205–227.

[11] Pai, P. F. (2007) Highly Flexible Structure: Modeling, Computation, and Experimentation. American Institute of Aeronautics and Astronautics, Inc., Reston.

[12] Sarpkaya, T. and Isaacson M. (1981). Mechanics of wave forces on offshore structures. Van Nostrand Reinhold Co.

[13] Borgman, L. E. (1967) Ocean wave simulation for engineering design. No. HEL-9-13. University of California Berkeley Hydraulic Engineering Lab.

[14] Goda, Y. (1979) A review of statistical interpretation of wave data, Report of the Port and Harbour Research Institute, **18**, 5-32.